Research Article

A Novel Dual-Band Four Port MIMO Antenna Design for 28/38 GHz Millimeter-Wave 5G Applications

Nermin Hamdan and Cetin Kurnaz

Abstract— **This paper presents an innovative dual-band Multiple-Input Multiple-Output (MIMO) antenna designed for millimeter-wave (mmWave) communication systems in fifth-generation (5G) technology. It operates across two frequency ranges: 26 to 31 GHz and 34.5 to 40 GHz. The antenna achieves a remarkable gain of 10.6 dBi at 28 GHz and an efficiency greater than 70%. At 38 GHz, it maintains a solid gain of 6.65 dBi and an efficiency of 50%. Simulation results show an average isolation of around -30 dB between the antenna elements. The diversity gain is estimated at about 10 dB, and the envelope correlation coefficient is nearly 10^{-6}, indicating enhanced performance over earlier antenna designs. The strong performance characteristics of this dual-band MIMO antenna highlight its potential as a leading option for mmWave 5G applications.**

Index Terms— **mmWave, 5G, MIMO, Microstrip antenna, CST.**

I. INTRODUCTION

WIRELESS COMMUNICATION technology has remarkably changed how we communicate and socialize since its inception. It helped us to transmit data over a distance without any cables—furthermore, the capability to communicate while on the move has progressed significantly. The several generations of wireless communication over time were one of the main reasons that led to a revolution in mobile communication. The rapid growth in connected devices and limited bandwidth has driven the evolution of wireless communication into fifth-generation (5G) technology. 5G seeks to improve mobile network data rates, scalability, connectivity, and energy efficiency. In the research fields of telecommunications, the 5G antenna design is one of the most sought-after topics. As technology develops, user demands also increase. To cope with this demand, millimeter-wave (mmWave) frequencies for unused spectrum are used in favor of the 5G.

NERMIN HAMDAN is with the Department of Electrical and Electronics Engineering, Ondokuz Mayıs University, Samsun, Turkey (e-mail: eng.nermin.hamdan@gmail.com).
https://orcid.org/0000-0002-5347-2832
ÇETİN KURNAZ, is with Department of Electrical and Electronics Engineering, Ondokuz Mayıs University, Samsun, Turkey, (e-mail: ckurnaz@omu.edu.tr).
https://orcid.org/0000-0003-3436-899X

The International Telecommunications Union (ITU) has classified the frequency ranges of 27.5-29.5 GHz, 33.4-36.5 GHz, 37-40 GHz, 47-50.2 GHz, and 59.3-71.1 GHz as part of the 5G mmWave spectrum [1]. 5G mobile communications are expected to operate primarily in the 26, 28, and 38 GHz because the absorption of electromagnetic waves in these bands in the atmosphere is low. 5G systems require higher capacity and large bandwidth. Microstrip patch antennas have many outstanding features, such as being lightweight and small, making them popular in wireless communications [2]. Nevertheless, MIMO (multiple input multiple output) antennas have consistently played a crucial role in wireless communication systems. In addition, they facilitate multipath propagation, enabling higher data rates and increased capacity, which are fundamental features of 5G technology [3]. One of the most sought-after research topics in telecommunication is the 5G antenna design, which needs continuous improvement. Utilizing the microstrip MIMO antenna enhances the channel capacity within the 5G system. MIMO is an antenna technology that utilizes several antennas to provide performance improvements. In contrast, a microstrip antenna has the advantages of being small, low-profile, easy to manufacture and integrate, and affordable compared to other antennas. Also, one patch can reinforce dual and triple resonant frequencies.

A. Literature Review

The literature has demonstrated several antenna solutions for 5G mmWave bands. The studies carried out to create a comparison source by examining the previous references and obtaining a better result for the antenna to be designed are briefly summarized in Table I.

B. Scope and Objective of the Study

This research aims to develop two 4 × 4 MIMO antenna configurations operating in the 28 GHz and 38 GHz frequency ranges. The antenna design aims to achieve a compact form factor while offering wide bandwidth and high gain. The MIMO antenna consists of four microstrip patches, which help increase the capacity of the wireless communication channel when a single antenna element is insufficient. MIMO is an essential aspect widely utilized in high-end 5G telecommunication systems. Therefore, the proposed antenna will incorporate MIMO technology to achieve improved performance.

TABLE I
A SUMMARY OF 5G MMWAVE BAND ANTENNAS PRESENTED IN
THE LITERATURE

Reference	Spectrum (GHz)	Key Highlights
[4]	(27.5 – 30); (37 – 39)	4×4 MIMO antenna design with -35 dB S_{11}, 7 dBi gain, and less than 0.004 Envelope Correlation Coefficient (ECC).
[5]	(26.65 - 29.2); (37 - 39.05)	A 2 × 2 MIMO antenna features a peak gain of 1.83 dBi, an S11 parameter of -35 dB, an isolation level lower than -20 dB, an envelope correlation coefficient (ECC) below 0.001, and an efficiency rate of 75%.
[6]	(27 - 28.5) ; (37 – 39)	4×4 MIMO antenna with S_{11} -24.59 dB, isolation value below -26 dB, antenna gain 8 dBi.
[7]	(26.6 - 39)	4×4 MIMO antenna with isolation value below -20 dB, ECC value below 0.002, maximum antenna gain 5.28 dBi.
[8]	(23 – 40)	4×4 MIMO antenna with isolation value below -20 dB, ECC value below 0.0014, maximum gain 10 dBi, efficiency above 70%.
[9]	(24.10 - 27.18); (33 – 40)	4 × 4 MIMO antenna with S_{11} -25 dB, isolation value below -16 dB, ECC value below 0.1, gain 3 dBi, efficiency above 75%, diversity gain (DG) value above 9.5.
[10]	(25 – 29); (35 – 45)	2 × 2 MIMO antenna with an isolation value below -20 dB and achieves a peak gain of 8.35 dBi.
[11]	(27.5 - 30.25); (37 – 40)	4 × 4 MIMO antenna with S_{11} below -20 dB, isolation value below -24 dB, ECC value below 0.014, gain 7.09 dBi.
[12]	(28); (38)	4×4 MIMO antenna with S_{11} -18 dB, ECC below 0.001, gain 7.9 dBi, efficiency over 85%.
[13]	(25.9 - 30.4); (36.4 - 40.2)	1 × 1 SISO antenna with s_{11} below -20 dB, gain 4.5 dBi, efficiency above 80%, efficiency over 96%.
[14]	(27.9 - 28.45); (37.5 - 38.5)	2 × 2 MIMO antenna with a maximum gain of 8.56 dBi, efficiency of 91%, ECC value below 0.0023, and diversity gain value of 9.99.

II. MATERIAL AND METHODS

A. The Fifth Generation

The advent of 5G technology signifies a substantial enhancement in data rate and bandwidth, concurrently mitigating battery consumption, expanding coverage, and addressing critical aspects such as latency, security, reliability, and cost efficiency. Spectrum allocation is a key challenge in 5G communications, a concern underscored by various studies [15]. 5G brings new spectrum opportunities that allow the operating bands to extend up to 52.6 GHz. 5G mmWave communication is divided into two frequency ranges: Frequency Range 1 (FR1) and Frequency Range 2 (FR2). FR1 covers frequency ranges between 450 MHz and 6000 MHz, while FR2 spans frequencies from 24.25 GHz to 52.6 GHz. These frequencies are further divided into three bands: low, mid, and high. The low band (below 1 GHz) provides broader coverage but lower data speeds, the mid-band (1 GHz to 6 GHz) balances coverage and speed, and the high band (24 GHz to 40 GHz) delivers faster speeds but with a reduced coverage area [16].

The frequency bands used by 5G depend on the country of use. Unlike the traditional lower bands found worldwide, other higher bands vary. The third-generation partnership project (3GPP) standard has selected the frequencies of 28 and 38 GHz as the Ka-band, with four standard supports in different countries. The mmWave spectrum is divided into frequency ranges, such as n257, n258, n260, and n261, each serving distinct applications [17]. The standard (n257) covers a range of 26.5 to 29.5 GHz for the U.S., Japan, and South Korea. At the same time, the standard (n261) is a subset of the band (n257) and covers a narrower range from 27.5 to 28.35 GHz. Europe and China's standard (n258) covers 24.25 to 27.5 GHz. Also, the standard (n260) for the U.S. covers 37 to 40 GHz [18].

B. Millimeter Wave

5G mobile communications standard recognizes the need for mmWave frequency bands. mmWave has shown great potential for increasing wireless data rates due to its high bandwidth. mmWave frequencies range from 30 to 300 GHz. The unused mmWave spectrum offers an excellent opportunity for additional broadband capacity and, thus, a better quality of service for users [19]. Several factors make 28/38 GHz among the existing mmWave the most suitable frequencies for 5G [20]. The Ka-band has been the subject of much research about the 5G mobile communications standard. A wide bandwidth is crucial to attain high data rates in the high-frequency range. Spectrum availability as many spectrum bands are underutilized, allowing several hundred megahertz to be assigned to 5G services. Regarding geographic harmony, the Ka-band is available in many countries. Since these bands are less affected by atmospheric absorption and attenuation, they are advantageous for cellular communications.

C. Microscript Antenna

The microstrip antenna (commonly called a patch antenna) is crucial in wireless communication technology today and is one of the most popular printed antennas. As illustrated in Fig. 1, the rectangular microstrip patch antenna comprises a radiation patch on one side, a dielectric substrate, and a ground plane on the other. A microstrip patch antenna has the advantages of being small, low-profile, easy to manufacture and integrate, and affordable over different types of antennas. An important design challenge is an antenna with a compact size and wide bandwidth that provides high gain and low S-parameter. Accurate impedance matching is essential in the design process of a microstrip patch antenna. Microstrip inset feed lines are employed to supply the antenna with a source. Several approaches can be used to analyze microstrip antennas, such as the transmission line approach, the cavity model, and the full-wave method. We opted for the transmission-line model, as it is widely recognized as the simplest and most used method among those mentioned. The antenna design process entails the creation of both the radiator patch and the feed line. The antenna's characteristics are significantly influenced by three essential parameters: the dielectric constant (ε_r), substrate thickness (h), and resonant frequency (f_r) [21].

According to Equation (1), the width of the antenna is determined as;

$$W = \frac{c}{2f_r\sqrt{\frac{(\varepsilon_r+1)}{2}}} \tag{1}$$

Here, c represents the speed of light.

According to Equation (2), the effective permittivity is determined.

$$\varepsilon_{eff} = \frac{1}{2}(\varepsilon_r + 1) + \frac{1}{2}(\varepsilon_r - 1)(1 + 12\frac{h}{w})^{\frac{-1}{2}} \quad (2)$$

The extension length (L_{eff}) is calculated according to Equation (3), as shown in Fig. 1.

$$L_{eff} = \frac{c}{2f_r\sqrt{\varepsilon_{eff}}} \quad (3)$$

The extension length resulting from the fringing field can be determined using Equation (4).

$$\Delta L = 0.412h\frac{(\varepsilon_{eff}+0.3)(\frac{W}{h}+0.264)}{(\varepsilon_{eff}-0.258)(\frac{W}{h}+0.8)} \quad (4)$$

According to Equation (5), the length of the patch is determined.
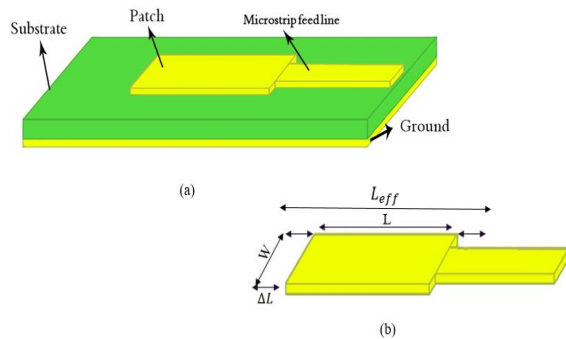
$$L = L_{eff} - 2\Delta L \quad (5)$$

Fig. 1. a) Microstrip antenna design, b) Antenna viewed from above.

D. Antenna Design

The presented study sought to design and optimize 4 × 4 MIMO antenna structures operating on different mmWave bands in a dual-band mode. This was initiated by analyzing the key features of a typical antenna and its parameters, which are used to identify its purpose and efficiency. As shown in Fig. 2, In the proposed design, a single antenna with an FR-4 dielectric substrate and a rectangular patch antenna were initially created as part of the proposed design of four elements. After that, the antenna's parameters underwent numerous procedures, continuously generated by Computer Simulation Technology (CST), aiming to identify and optimize the antenna's strengths and weaknesses. CST Studio Suite is an advanced 3D electromagnetic simulation software package that provides a comprehensive array of tools for conducting electromagnetic analysis and simulations [22]. It is an essential tool for engineers and researchers involved in various electromagnetic applications.

These procedures included adding and constantly modifying up to four slots and one slot on the patch antenna and the ground. After reaching the last design of the antenna with the most satisfactory characteristics, the 5G MIMO antenna was constructed by implementing four identical elements arranged

circularly, in which they have minimal interference with each other.

FR-4 was chosen as the substrate for this design due to its widespread availability and favorable low-loss characteristics. It aligns perfectly with our design requirements with a dielectric constant of 4.4, a thickness of 1.55 mm, and a dielectric loss tangent of 0.02. The patch and ground plane are made of copper, featuring a thickness of 0.035 mm. The antenna is fed using a 50 Ω SMA connector. By applying Equations (1-5), the patch's precise length and width were calculated. Table II provides a comprehensive list of the antenna's dimensions.
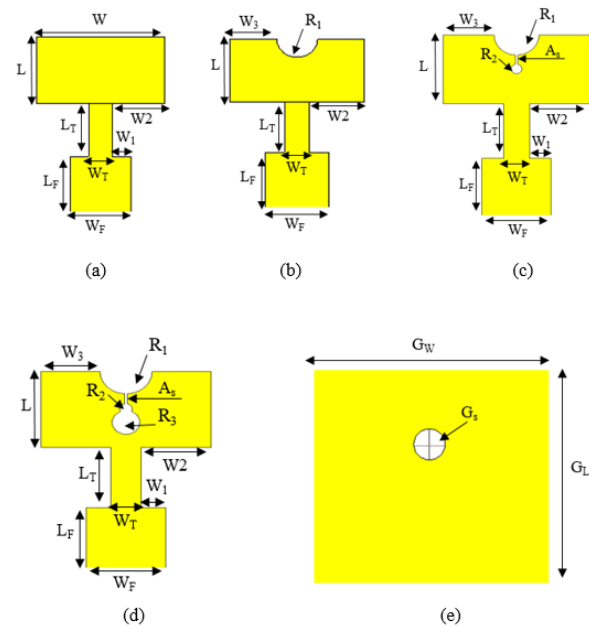

Fig. 2. A comprehensive overview of the design stages for the single antenna is presented: a) Stage-1, b) Stage-2, c) Stage-3, d) Stage-4, e) Stage-5 (note that only the ground layer in Stage-4 was modified).

TABLE II
GENERAL DIMENSIONS OF THE PROPOSED SINGLE ANTENNA

Parameter	Dimension [mm]	Parameter	Dimension [mm]
L	2.16	W	3.26
L_T	1.35	W_T	0.58
L_F	1.47	W_F	1.53
W_1	0.47	W_2	1.34
W_3	1	R_1	0.63
R_2	0.2	R_3	0.35
A_s	0.1 x 0.23	G_s	0.63
G_L	8.75	G_W	8.75

A ground slot technique was employed to enhance the bandwidth of the antennas, as shown in studies [23-25]. The findings indicate that these slots enhance impedance matching with minimal impact on the antenna's radiation properties. Similarly, a patch slot approach was applied to boost antenna performance, as described in [26]. Results reveal that, when utilized appropriately, the slots can extend the electrical length

and generate more focused radiation with higher gain. The shape of the slots can be rectangular [27], triangular [28], circular [29], etc. As shown in Fig. 2, numerous procedures were applied to the rectangular patch antenna to improve its parameters. One of these procedures is to add a circle to the patch antenna's ground and change the circle's size and position. During the antenna design process, enhancements can be applied to traditional antennas by incorporating parasitic elements, slots, notches, and repositioning feed points to boost bandwidth, directivity, and gain, among other performance metrics [30]. These operations can be carried out by trial-and-error method or by using "Parametric Analysis" and "Optimization Techniques." In this study, the trial-and-error method was preferred. Once the last design of the antenna, with the most satisfactory characteristics, was achieved, the 5G MIMO antenna was constructed by implementing four identical elements arranged circularly with an 18 x 18 mm^2 overall size in which they have minimal interference. Fig. 2 depicts the preliminary design of the MIMO antenna, which was subsequently refined to meet U.S. standards, as represented in Fig. 3.
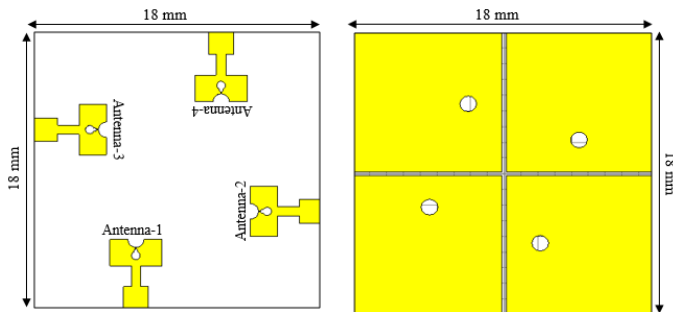

Fig. 3. Antenna geometry, a) front, b) back side of the antenna

It is evident that the dimensions and positioning of the slot in the ground, the spacing between each antenna patch, as well as both the length and width of the ground and patch antenna play a crucial role in determining how well the operating frequency is matched.

III. RESULTS AND DISCUSSION

A. The Result of the Single Antenna

Fig. 4 depicts the single antenna, designed in stages to reach the final design. In Stage-1, the initial design is presented, and the propagation band needs to be modified. In Stage-2, the design has been modified by adding a slot in the middle. A similar slot has been added to the back in Stage-3, and the results have been better. As the slot implementation showed promising results, another three slots were implemented in the middle of the patch. Overall, the adjustments of the slots managed to make the single antenna operate from 25 to 29 GHz and from 34 to 41 GHz based on -10 dB as a S_{11}.
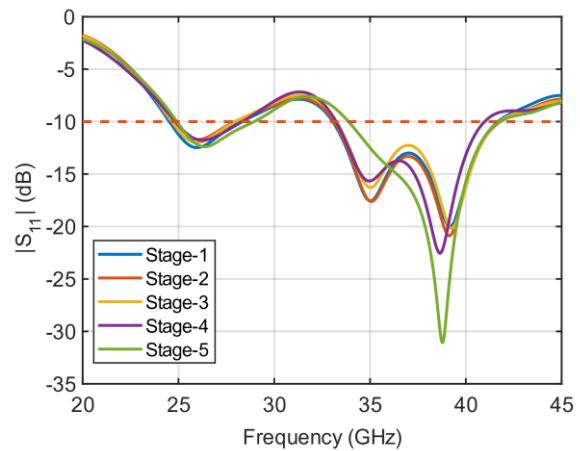

Fig. 4. The S_{11} parameter for each stage of a single antenna design

B. The Result of the MIMO Antenna

Fig. 5 presents the S-parameters of the proposed antenna, showing that all propagate within the dual band and exhibit minimal differences in their S-parameter values. The peak S-parameter values for the MIMO antenna reach -18 dB at 28 GHz and -33 dB at 38 GHz. Furthermore, the bandwidth is 5 GHz for the 28 GHz band and 5.5 GHz for the 38 GHz band.
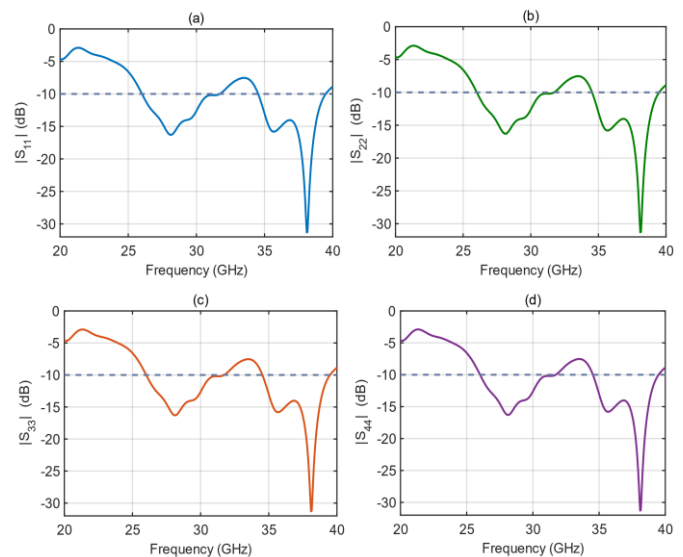

Fig. 5. The S-parameters of the designed MIMO antenna

Fig. 6 illustrates the level of isolation between the radiating patches. The diagram shows that the average isolation at 28 GHz and 38 GHz is below -20 dB and -30 dB, respectively. This is due to the arrangement of the patches to ensure low mutual coupling.
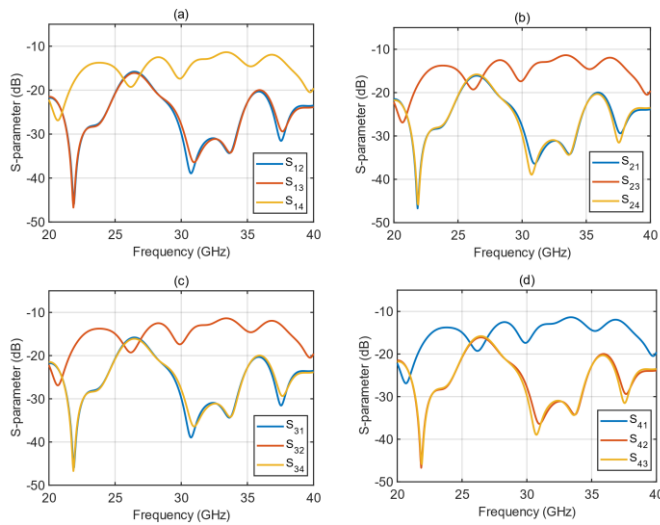
Fig. 6. Isolation between ports of the patch antenna

Fig. 7 shows the 3D simulated radiation patterns for individual elements of the MIMO antenna at 28 GHz, revealing a peak directional gain of 10.6 dBi.
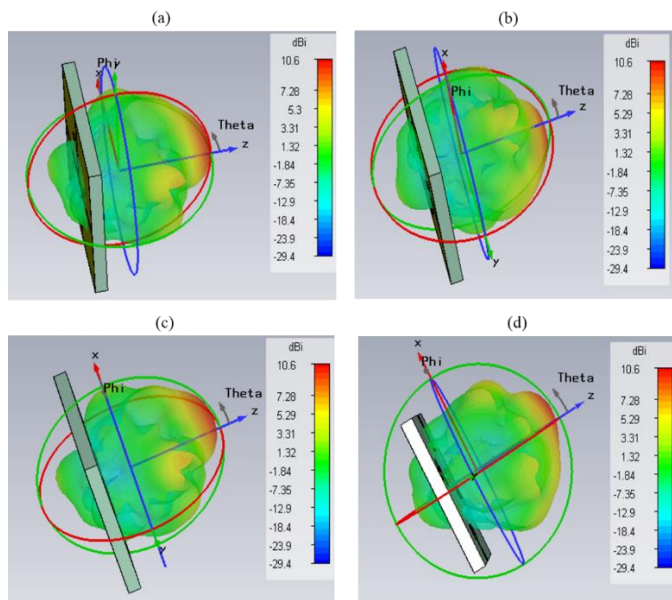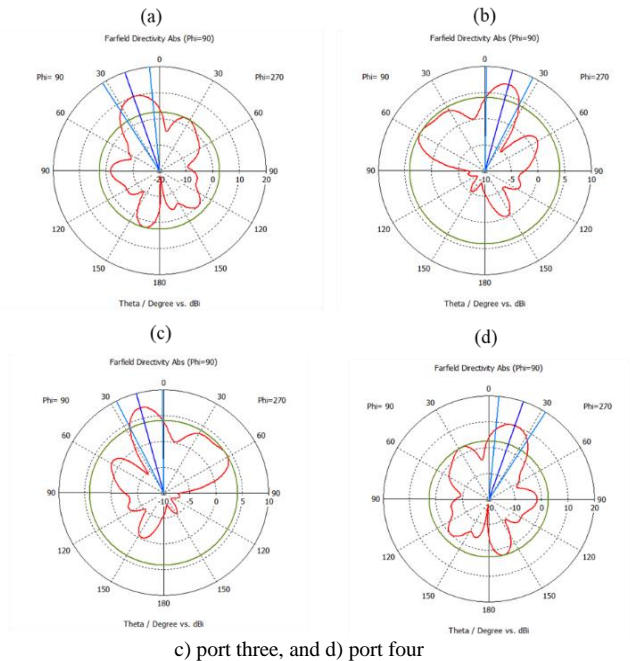

Fig. 7. The 3D radiation patterns at 28 GHz for a) port one, b) port two, c) port three, and d) port four

While Fig. 8 illustrates the radiation pattern in polar form, indicating that the first and fourth ports exhibit a main lobe magnitude of 10.1 dBi each, the second and third ports display a main lobe magnitude of 7.12 dBi. Additionally, nearly all elements demonstrate a directional pattern.

Fig. 8. The polar radiation patterns at 28 GHz for a) port one, b) port two,

c) port three, and d) port four

Fig. 9 illustrates the 3D simulated radiation patterns for the finalized MIMO antenna at 38 GHz, showing a peak directional gain of 6.65 dBi for each element.
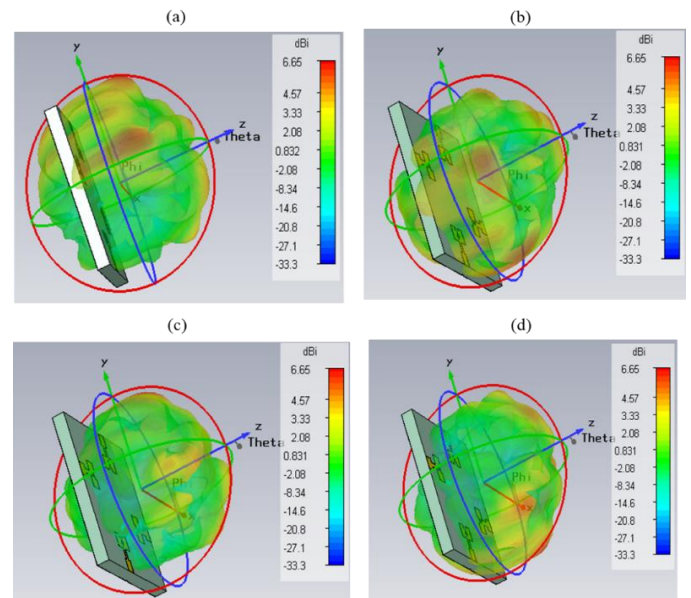

Fig. 9. The 3D radiation patterns at 38 GHz for a) port one, b) port two, c) port three, and d) port four

Whereas Fig. 10 displays the radiation pattern in the polar form, the first and fourth ports have a main lobe magnitude of 4.03 dBi, while other ports have a main lobe of 4.06 dBi, and almost all elements show a semi-directional pattern.
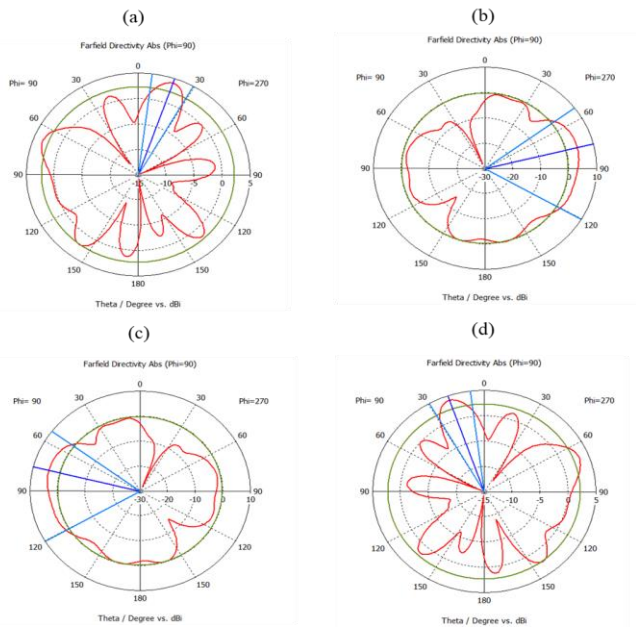
Fig. 10. The polar radiation pattern at 38 GHz of a) the first port, b) the second port, c) the third port, d) the fourth port

Fig. 11 shows the efficiency of each element in the designed MIMO antenna. At 28 GHz, the total efficiency exceeds 70%, while at 38 GHz, it is approximately 50% across all ports.
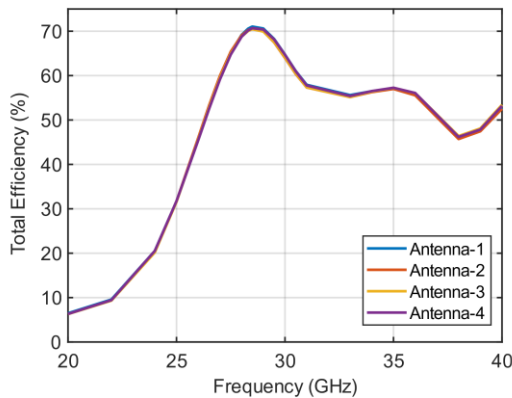

Fig. 11. The efficiency of each port of the MIMO antenna.

Fig. 12 illustrates the ECC of the design between each port at both 28 and 38 GHz frequencies. Additionally, Table III presents a detailed breakdown of the ECC values between each port for both frequency bands. When Fig. 12 and Table III are evaluated together, it is seen that for 28 GHz, the lowest ECC value was 3.39×10^{-6} for S_{12}/S_{21}, while the highest ECC value was 4.52×10^{-3} for S_{23}/S_{32}. For 38 GHz, the lowest ECC value was 6.13×10^{-6} for S_{13}/S_{31}, while the highest ECC value was 1.72×10^{-3} for S_{23}/S_{32}.
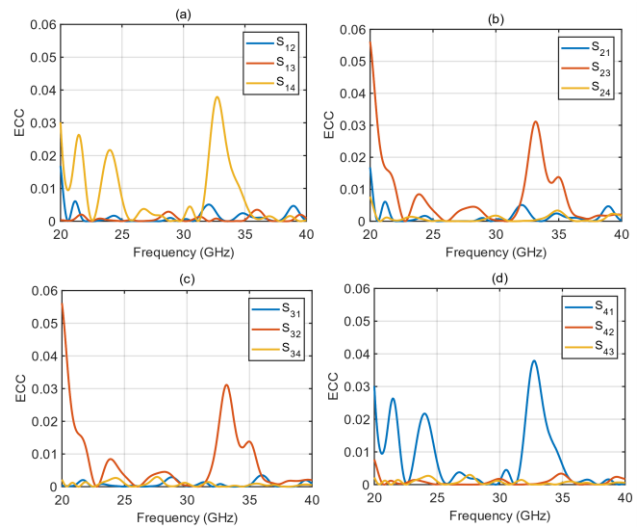

Fig. 12. The performance of the antenna's ECC

TABLE III
THE ECC VALUES BETWEEN EACH PATCH ANTENNA PORT

ECC	28 GHz	38 GHz
S_{12} / S_{21}	3.39×10^{-6}	6.84×10^{-4}
S_{13} / S_{31}	1.10×10^{-3}	6.13×10^{-6}
S_{14} / S_{41}	1.81×10^{-3}	1.95×10^{-4}
S_{23} / S_{32}	4.52×10^{-3}	1.72×10^{-3}
S_{24} / S_{42}	8.41×10^{-6}	3.01×10^{-5}
S_{34} / S_{43}	1.92×10^{-3}	1.01×10^{-5}

Similarly, diversity gain (DG) is another important performance indicator. As depicted in Fig. 13, the DG approaches 10 dB within the target frequency bands of 28 and 38 GHz.
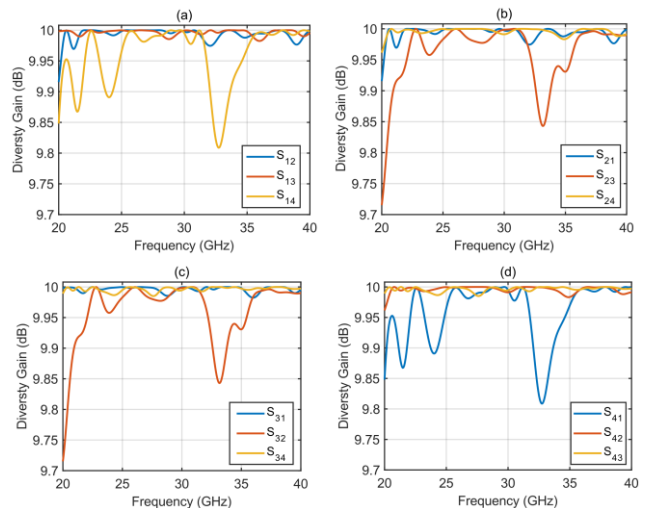

Fig. 13. The performance of DG for the designed antenna

TABLE IV
COMPARISON WITH ANTENNA IN OTHER STUDIES

| Ref.	Spectrum (GHz)	Bandwidth	Antenna Elements	Antenna size L x W (mm²)	S₁₁ dB	Gain dBi	Efficiency %	Isolation dB	ECC
[4]	27.5-30 37-39	2.5 GHz 2 GHz	4 × 4	19.25 × 25	<-30	7 5	-	-	<0.004
[5]	26.65- 29.2 37-39.05	2.55 GHz 2.05 GHz	2 × 2	14 ×26	-35	1.27 1.83	75	<-20	0.001
[6]	27-28.5 37-39	1.5 GHz 2 GHz	4 × 4	55 ×110	-21.57 -24.59	7.95 8	<70	-26	7650.0000
[7]	26.6-39	12.4 GHz	4 × 4	30 × 25	<-15	5.2	70	<-20	0.002
[8]	23-40	17 GHz	4 × 4	80 × 80	-25	11	>70	>-20	<0.0014
[9]	24.10-27.18 33-40	3.08 GHz 7 GHz	4 × 4	24 × 20	-25	3	75	>-16	<0.1
[10]	25-30 35-45	5 GHz 10 GHz	2 × 2	21.96 × 16.71	>-35	8.35 6.48	80	<-20	-
[11]	27.5-30.25 37-40	2.75 GHz 3 GHz	4 × 4	14 × 14	<-28 <-17	7.09 3.43	55	<-24 <-17	0.014
[12]	27.6–28.6 37.4–38.6	1 GHz 1 GHz	4 × 4	20 × 24	-18 -20	7.1 7.9	<85	<-25	<0.001
[13]	25.9- 30.4 36.4 - 40.2	5.4 GHz 3.8 GHz	1× 1	12×12	<-20	4.5	80	-	-
[14]	27.9-28.45 37.5-38.5	0.55 GHz 1 GHz	2 × 2	10 × 17	-25 -15	7.46 8.56	77	-23.3 -21.4	0.0023
Proposed	26-31 34.5-40	5 GHz 5.5 GHz	4 × 4	18 × 18	-18 -33	10.6 6.65	>70 >50	-20 -30	<0.00001
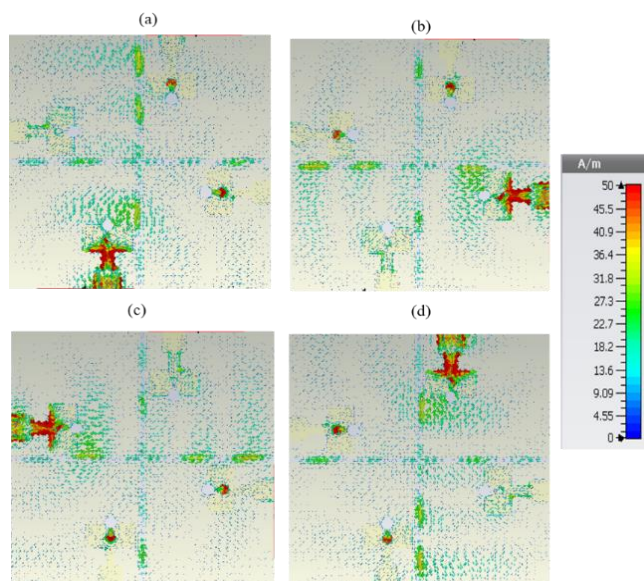
Fig. 14. The surface current of a) the first port, b) the second port, c) the third port, d) the fourth port of the second design at 28 GHz

Figures 14 and 15 depict the surface current distribution on each patch of the MIMO antenna design at 28 GHz and 38 GHz, respectively. The results indicate a high current intensity along the connecting strips of the circular slots positioned at the center of the patch. Consequently, both the slot and the connecting strips above the feed significantly aid in achieving operation within the mmWave band. Additionally, the current distribution pattern on the surface suggests minimal interaction between the patches, as each patch is positioned at a 90-degree offset from its neighbors.

IV. DISCUSSION

Table IV presents a comparison between the proposed antenna and those discussed in previous studies. The literature review reports various antenna designs operating at 28 and 38 GHz bands. It also includes various designs with different elements, such as 1 × 1, 2 × 2, and 4 × 4. Furthermore, we have considered the sizes of other designs as one of our primary goals is to design a 4 × 4 MIMO antenna that is small compared to

other designs. In addition, we have provided a detailed analysis of MIMO performance, including isolation, DG, and ECC between ports. Accordingly, the study presents MIMO antennas as significantly more performant than other antennas.
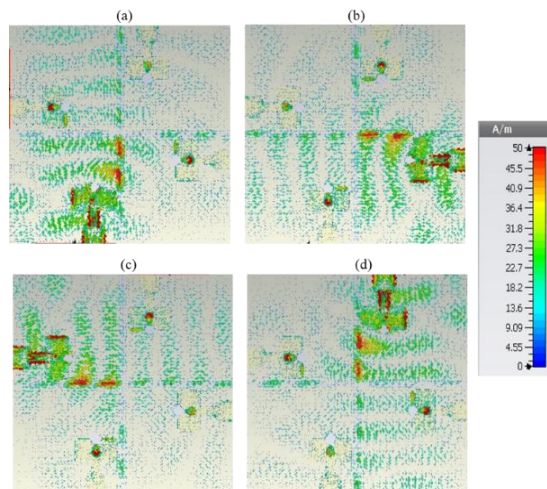

Fig. 15. The surface current of a) the first port, b) the second port, c) the third port, d) the fourth port of the antenna at 38 GHz

V. CONCLUSION

This study focuses on designing a 4×4 MIMO antenna that operates in a dual-band mode across various mmWave frequencies. Specifically, the antenna functions within the frequency ranges of 26 to 31 GHz and 34.5 to 40 GHz. It achieves a high gain of 10.6 dBi at 28 GHz and 6.65 dBi at 38 GHz, alongside radiation efficiencies exceeding 70% at 28 GHz and over 50% at 38 GHz, facilitating effective signal transmission and reception. The antenna exhibits strong isolation, with average isolation values of -20 dB in the first band (26 - 31 GHz) and -30 dB in the second band (34.5 - 40 GHz). The diversity gain, which approaches 10 dB, highlights the antenna's capability to focus radiation on the desired direction, further enhancing its performance. Moreover, the ECC is exceptionally low, at less than 1×10^{-6}, which indicates reliable communication with minimal error. Overall, the performance attributes of this antenna render it highly suitable for mmWave 5G applications.

REFERENCES

[1] M.I. Khattak, A. Sohail, U. Khan, Z. Barki, and G. Witjaksono, "Elliptical slot circular patch antenna array with dual-band behavior for future 5G mobile communication networks". Progress In Electromagnetics Research C, vol. 89, pp. 133-147, 2019.

[2] O.S. Zakariyya, B.O. Sadiq, O.A. Abdulrahman, and A.F. Salami, "Modified edge fed Sierpinski carpet miniaturized microstrip Patch antenna", Nigerian Journal of Technology, vol. 35, no. 3, pp. 637-641, 2016.

[3] M. Rahman, M.N. Jahromi, S.S. Mirjavadi, and A.M. Hamouda, "Compact UWB band-notched antenna with integrated bluetooth for personal wireless communication and UWB applications", Electronics, vol. 8, no. 8, 2019.

[4] D.T.T. Tu, N.G. Thang, N.T. Ngoc, N.T.B. Phuong, and V. Van Yem, "28/38 GHz dual-band MIMO antenna with low mutual coupling using novel round patch EBG cell for 5G applications". In 2017 International

Conference on Advanced Technologies for Communications, 18-20 October, EEE, Quy Nhon, Vietnam, 2017, pp. 64-69.

[5] M.N. Hasan, S. Bashir, and S. Chu, "Dual band omnidirectional millimeter wave antenna for 5G communications", Journal of Electromagnetic Waves and Applications, vol. 33, no. 12, pp. 1581-1590, 2019.

[6] H.M. Marzouk, M.I. Ahmed, and A.H.A. Shaalan, "Novel dual-band 28/38 GHz MIMO antennas for 5G mobile applications", Progress In Electromagnetics Research C, vol. 93, pp. 103-117, 2019.

[7] M. Shuhrawardy, M.H.M. Chowdhury, and R. Azim, "A four-element compact wideband MIMO antenna for 5G applications". In 2019 International Conference on Electrical, Computer and Communication Engineering (ECCE), 07-09 February, Cox'sBazar, Bangladesh, 2019, pp. 1-5.

[8] D.A. Sehrai, M. Abdullah, A. Altaf, S.H. Kiani, F. Muhammad, M. Tufail, and S. Rahman, "A novel high gain wideband MIMO antenna for 5G millimeter wave applications", Electronics, vol. 9, no. 6, pp. 1-13, (2020).

[9] A. Desai, C.D. Bui, J. Patel, T. Upadhyaya, G. Byun, and T.K. Nguyen, "Compact wideband four element optically transparent MIMO antenna for mm-wave 5G applications", IEEE Access, vol. 8, 194206-194217, 2020.

[10] M.L. Hakim, M.J. Uddin, and M.J. Hoque, "28/38 GHz Dual-Band Microstrip Patch Antenna with DGS and Stub-Slot Configurations and Its 2×2 MIMO Antenna Design for 5G Wireless Communication", 2020 IEEE Region 10 Symposium (TENSYMP) 05-07 June, Dhaka, Bangladesh, 2020, pp. 56-59.

[11] S. Saleem, S. Kumari, D. Yadav, and D. Bhatnagar, "Compact millimeter-wave MIMO (multiple-input multiple-output) antenna for 5G Applications", In 2021 IEEE Indian Conference on Antennas and Propagation (InCAP) 13-16 December, IEEE, Jaipur, Rajasthan, India, 2021, pp. 1035-1038.

[12] K. Raheel, A. Altaf, A. Waheed, S.H. Kiani, D.A. Sehrai, F. Tubbal, and R. Raad, "E-shaped H-slotted dual band mmWave antenna for 5G technology", Electronics, vol. 10, no. 9, pp. 1-10, 2021.

[13] A.R. Sabek, A.A. Ibrahim, and W.A. Ali, "Dual-band millimeter wave microstrip patch antenna with stubresonators for 28/38 GHz applications", In Journal of Physics: Conference Series, vol. 2128, no. 1, 2021.

[14] S. Chaudhary, and A. Kansal, "Compact high gain 28, 38 GHz antenna for 5G communication", International Journal of Electronics, vol. 110, no. 6, pp. 1028-1048. 2022.

[15] A. Osseiran, F. Boccardi, V. Braun, K. Kusume, P. Marsch, M. Maternia, and M. Fallgren, "Scenarios for 5G mobile and wireless communications: the vision of the METIS project", IEEE Communications Magazine, vol. 52, no. 5, pp. 26-35, 2014.

[16] 3rd Generation Partnership Project (3GPP). "Technical Specification Group Radio Access Network; NR; Frequencies and Operating Bands." 3GPP TS 38.101-1.

[17] FCC, "America's 5G future," Federal Commun. Commission. https://www.fcc.gov/5G (accessed March 20, 2024).

[18] M. L. Hakim, M. T. Islam and T. Alam, "Incident Angle Stable Broadband Conformal mm-Wave FSS for 5G (n257, n258, n260, and n261) Band EMI Shielding Application," IEEE Antennas and Wireless Propagation Letters, vol. 23, no. 2, pp. 488-492, Feb. 2024, doi: 10.1109/LAWP.2023.3326868.

[19] S. Rangan, T.S. Rappaport, and E. Erkip, "Millimeter-wave cellular wireless networks: Potentials and challenges", Proceedings of the IEEE, vol. 102, no. 3, pp. 366-385, 2014.

[20] N. Al-Falahy, and O.Y. Alani, Millimetre wave frequency band as a candidate spectrum for 5G network architecture: A survey, Physical Communication, vol. 32, pp. 120-144, 2019.

[21] C.A. Balanis, "Antenna Theory: Analysis and Design", Willey-Inter Science, (2005).

[22] CST Studio Suite, https://www.3ds.com/products/simulia/cst-studio-suite, (accessed September 29, 2024).

[23] J.J. Golezani, M. Abbak, I. Akduman I. "Modified directional wide band printed monopole antenna for use in radar and microwave imaging applications", Prog Electromagn Res Lett. vol.33, pp.119–129, 2012. doi:10.2528/PIERL1205280

[24] M.H. Bah, J. Hong, DA. Jamro, "Ground slotted monopole antenna design for microwave breast cancer detection based on time reversal MUSIC", Progress in Electromagnetics Research C, vol. 59, pp.117–126, 2015. doi:10.2528/PIERC1508290.

[25] Z. Wani, D. Kumar, "Dual-band-notched antenna for UWB MIMO applications", Int J Microwave Wireless Technolog. vol.35, pp.1–6, 2015.

[26] M.T. Islam, M.Z Mahmud, N. Misran, J. Takada, M. Cho, "Microwave breast phantom measurement system with compact side slotted directional antenna", IEEE Access, vol.5, pp.5321-5330, 2017.

[27] S. Sarkar, A.D. Majumdar, S. Mondal, S. Biswas, D. Sarkar, P.P. Sarkar, "Miniaturization of rectangular microstrip patch antenna using optimized single-slotted ground plane", Microwave and Optical Technology Letter, vol. 53, no. 1, pp.111–115, 2011. doi:10.1002/mop.

[28] M.A. Ullah, F.B. Ashraf, T. Alam, M.S. Alam, S. Kibria, M.T. Islam, "A compact triangular shaped microstrip patch antenna with triangular slotted ground for UWB application", Proceedings of the International Conference on Innovations in Science, Engineering and Technology (ICISET); Dhaka, Bangladesh, 2016.

[29] I. Ganesan, I. Paulkani,   "Design of ultra wideband circular slot antenna for emergency communication applications", e-Prime-Advances in Electrical Engineering, Electronics and Energy, vol. 6, 2023.

[30] A.R. Celik, M.B. Kurt, "Development of an ultrawideband, stable and high-directive monopole disc antenna for radar-based microwave imaging of breast cancer", Journal of Microwave Power and Electromagnetic Energy,   vol.52,   no.2,   pp.75-93,   2018, DOI:10.1080/08327823.2018.1458692

BIOGRAPHIES

NERMIN HAMDAN received a bachelor's degree in computer and communication Engineering from Al-Azhar University in Palestine with a degree of excellence. In 2019, she worked at the Engineering Department at Al-Azhar University as a teacher's assistant. In 2020, she got accepted into the Turkey scholarship to pursue her master's degree in communication engineering at Ondokuz Mayıs University, Institute of Science and Technology, Department of Electrical and Electronics Engineering. She successfully completed her master's degree in 2023.

CETIN KURNAZ received his B.Sc. degree in Electrical and Electronic Engineering from the Ondokuz Mayıs University in 1999. He received an M.Sc. in Electrical and Electronics Engineering from the Ondokuz Mayıs University in 2002. He received a Ph.D. in Electrical and Electronics Engineering from the Ondokuz Mayıs University in 2009. He is currently working as a Professor of Electrical and Electronics Engineering at Ondokuz Mayıs University. His research interests include Electromagnetic Fields, Microwave Techniques, Telecommunications, and Digital Signal Processing.